

# Galerkin Boundary Integral Method for Evaluating Surface Derivatives

L. J. Gray\*      D. Maroudas<sup>†</sup>      M. N. Enmark<sup>†</sup>

February 24, 1998

## Abstract

A Galerkin boundary integral procedure for evaluating the complete derivative, *e.g.*, potential gradient or stress tensor, is presented. The expressions for these boundary derivatives involve hypersingular kernels, and the advantage of the Galerkin approach is that the integrals exist when a continuous surface interpolation is employed. As a consequence, *nodal* derivative values, at smooth surface points or at corners, can be obtained directly. This method is applied to the problem of electromigration-driven void dynamics in thin film aluminum interconnects. In this application, the tangential component of the electric field on the boundary is required to compute the flux of atoms at the void surface.

**Key words.** boundary integral method, surface derivatives, hypersingular integrals, Laplace equation, electromigration.

## 1 Introduction

After a problem has been solved by means of the boundary integral method, the normal derivative – *e.g.*, normal flux component in potential theory or traction in elasticity – is known everywhere on the boundary. Some applications, however, require knowledge of

---

\*Computer Science and Mathematics Division, Oak Ridge National Laboratory, Oak Ridge, TN 37831

<sup>†</sup>Department of Chemical Engineering, University of California, Santa Barbara, CA 93106

the complete surface derivatives, *e.g.*, electric field or the full stress tensor. The tangential components can be expressed as boundary integrals of known quantities, but numerical evaluation is complicated by the presence of hypersingular kernel functions. Existence of the integral requires that the function (*e.g.*, potential, displacement) multiplying the hypersingular kernel be *differentiable* ( $C^1$ ) at the node (Gray 1991; Krishnasamy, Rizzo and Rudolphi 1991; Martin and Rizzo (1989,1996)), and this interpolation constraint is the source of the difficulty.

Previous work on this topic, mostly in the context of evaluating the surface stress tensor in elasticity, has taken three paths. The earliest work employed finite differencing (Cruse and Van Buren 1971; Rizzo and Shippy 1968) or differentiation of the shape functions (Sladek and Sladek 1986) to obtain the necessary derivatives of displacement. While simple, the drawback of this approach is, not surprisingly, loss of accuracy, as the tangential components are less accurate than the known or computed normal component. The second approach is to attack the hypersingular integral directly. Calculations employing  $C^1$  Overhauser splines (Hildenbrand and Kuhn 1992) have been successful, but these elements are difficult to work with and are computationally expensive, especially in three dimensions. Hermite elements (Rudolphi 1989; Watson 1986) are a possible alternative, but this approximation is not in widespread use, again due to computational cost. An additional important drawback of the direct approach is that the implementations are generally applicable only for smooth surfaces (Fiedler 1995). Evaluation of hypersingular integrals at corners and edges involves interpolation constraints that are generalizations of the  $C^1$  condition for smooth surfaces, and these conditions are difficult to incorporate numerically (Gray 1994).

The third class of methods is indirect techniques, which in some manner bypass the hypersingular integral and the differentiability condition. In the 'non-conforming' approach, derivatives are evaluated at points interior to the element (Guiggiani 1993; Lutz, Gray and Ingraffea 1990; Zhao 1997), where all functions are differentiable the hypersingular integral exists. However, the nodal values must then be obtained by an additional approximate interpolation. A completely non-hypersingular scheme, and perhaps the best available method for nodal derivatives, is the 'displacement gradient' approach of Okada, Rajiyah and Atluri (1988,1989). This technique formulates an additional, non-hypersingular, system of boundary integral equations for the gradient, from which the stress can be computed. Its main advantage is that nodal values are computed using standard and relatively straightforward numerical methods, Matsumoto, Tanaka and Hirata 1993. However, a completely new boundary integral formulation, *i.e.*, new kernel functions, must be implemented and solved.

In this paper, a general algorithm for direct evaluation of nodal surface derivatives, using

standard continuous ( $C^0$ ) elements, is presented (section 2). This is accomplished by employing a Galerkin treatment (Kane 1994) of the integral equations that define the derivatives. The Galerkin formulation uses a second integration over the boundary, and this extra integration allows the hypersingular integral to be defined for a  $C^0$  interpolation. This approach is similar to displacement gradients in that a system of equations for the surface derivatives everywhere on the boundary is constructed. However, the Galerkin method does not require a new integral equation formulation, and it should be appreciably faster. In two dimensions, the tangential derivative can be computed directly, as opposed to computing the gradient components, and thus there are half as many unknowns. In three dimensions there is not a unique tangent vector, and thus the Galerkin method will generally have to compute gradient components. However, in elasticity (or other vector problems), the method can work with the stress tensor components directly; in this case, there are only six unknowns (from the symmetry of the tensor) compared to the nine displacement gradients. Moreover, the Galerkin coefficient matrix is sparse and symmetric, and the system of equations ‘naturally’ terminates at boundary corners.

As a consequence, the primary advantage of this approach over displacement gradient is reduced computational effort. Two additional advantages are that tangential derivatives at boundary corners can be directly evaluated, and that only the usual singular and hypersingular equations are required.

This algorithm was motivated by, and is applied to, a problem of physical and technological interest: electromigration-driven void dynamics in aluminum thin films. These films are used for device interconnections in modern integrated circuits. Electromigration-induced interconnect failure is one of the most serious reliability problems in microelectronics, see *e.g.*, Bower and Freund 1995; Maroudas 1995; Maroudas and Pantelides 1995, and references therein. Modeling the effect of an electric field on the void requires solving a boundary value problem involving Laplace’s equation for the electrostatic potential, and then computing the tangential component of the electric field on the void surface. This tangential component is responsible for driving atomic electromigration on the surface. As the exact solution is not known in the electromigration calculations, the boundary integral results are validated by comparing with solutions obtained with the finite element method employing highly refined meshes (section 3).

## 2 Calculation of Tangential Derivatives

Although presented here in the context of the Laplace equation, the algorithm for calculating surface derivatives is a general scheme and should prove useful in other applications,

*e.g.*, calculation of the surface stress tensor in mechanics problems. The boundary integral equations for the two dimensional Laplace equation,  $\nabla^2\phi = 0$  in the domain  $\mathcal{D}$ , are the equations for surface potential  $\phi$

$$\phi(P) + \int_{\Gamma} \phi(Q) \frac{\partial G}{\partial \mathbf{n}}(P, Q) dQ = \int_{\Gamma} G(P, Q) \frac{\partial \phi}{\partial \mathbf{n}} dQ , \quad (1)$$

and the equation for surface normal flux component  $\partial\phi/\partial\mathbf{n}$

$$\frac{\partial\phi(P)}{\partial \mathbf{N}} + \int_{\Gamma} \phi(Q) \frac{\partial^2 G}{\partial \mathbf{N} \partial \mathbf{n}}(P, Q) dQ = \int_{\Gamma} \frac{\partial G}{\partial \mathbf{N}}(P, Q) \frac{\partial \phi}{\partial \mathbf{n}}(Q) dQ . \quad (2)$$

Here  $\mathbf{n} = \mathbf{n}(Q)$ ,  $\mathbf{N} = \mathbf{N}(P)$  denote the unit outward normal on the boundary curve  $\Gamma$  of the domain  $\mathcal{D}$ , and  $P$  and  $Q$  denote points on  $\Gamma$ . These equations are customarily written with a ‘solid angle’ coefficient multiplying the leading term, Kane 1994. However, it is assumed that the singular integrals are defined in terms of a limit to the boundary, thus resulting in a coefficient of 1, Lutz and Gray 1993. Although the fundamental solution is usually taken as the point source potential,

$$G(P, Q) = -\frac{1}{2\pi} \log \|Q - P\| . \quad (3)$$

the electromigration calculations presented below will employ an approximate Green’s function tailored to this particular problem.

Using Eq. (1) and/or Eq. (2), the boundary value problem can be solved, and the potential and normal flux are then known everywhere on the boundary. Replacing  $\mathbf{N}$  with the unit tangent  $\mathbf{T}$  in Eq. (2), the tangential component of the electric field can be expressed as

$$\frac{\partial\phi(P)}{\partial \mathbf{T}} = \int_{\Gamma} \left[ \frac{\partial G}{\partial \mathbf{T}}(P, Q) \frac{\partial \phi}{\partial \mathbf{n}}(Q) - \phi(Q) \frac{\partial^2 G}{\partial \mathbf{T} \partial \mathbf{n}}(P, Q) \right] dQ . \quad (4)$$

However, as discussed in the introduction, direct evaluation of this equation is difficult because the hypersingular integral requires that  $\phi$  be differentiable at the ‘collocation point’  $P$ . Thus, unless a  $C^1$  interpolation was employed in solving the problem, direct evaluation of Eq. (4) *at a nodal point* is not possible. The differentiability condition does not arise if Eq. (4) is implemented via a Galerkin approximation. In this approach, the shape functions  $\psi_k(P)$  are employed as weighting functions, enforcing the tangential derivative equation in the form

$$\int_{\Gamma} \psi_k(P) \frac{\partial\phi(P)}{\partial \mathbf{T}} dP = \int_{\Gamma} \psi_k(P) \int_{\Gamma} \left[ \frac{\partial G}{\partial \mathbf{T}}(P, Q) \frac{\partial \phi}{\partial \mathbf{n}}(Q) - \phi(Q) \frac{\partial^2 G}{\partial \mathbf{T} \partial \mathbf{n}}(P, Q) \right] dQ dP . \quad (5)$$

In effect, the added integration over  $P$  counterbalances the extra differentiation with respect to  $P$ , and thus the hypersingular integral will exist even with a  $C^0$  interpolation of the potential. Note that this approach sets up a system of algebraic equations for the derivative values: the equation centered at a particular node  $P_0$  ( $\psi_k(P_0) = 1$ ) will necessarily involve values at all ‘neighboring’ nodes, *i.e.*, nodes belonging to elements where  $\psi_k(P_0) \neq 0$ . Thus, Eq. (5) represents coupled equations for  $d\phi/d\mathbf{T}$  on the boundary. However, unlike with the displacement gradient method, this system of equations naturally terminates at boundary corners or edges (this will be discussed in more detail below). This aspect is advantageous for problems in which the tangential derivative is not needed everywhere on the boundary. Moreover, the coefficient matrix (left-hand side of Eq. (5)) is trivial to compute: it is symmetric, involves only “nearest neighbor interactions” (the shape functions will generally have limited support), and the non-zero elements simply require the integration of a pair of shape functions. The evaluation of the right hand side of Eq. (5), however, will be a relatively expensive calculation.

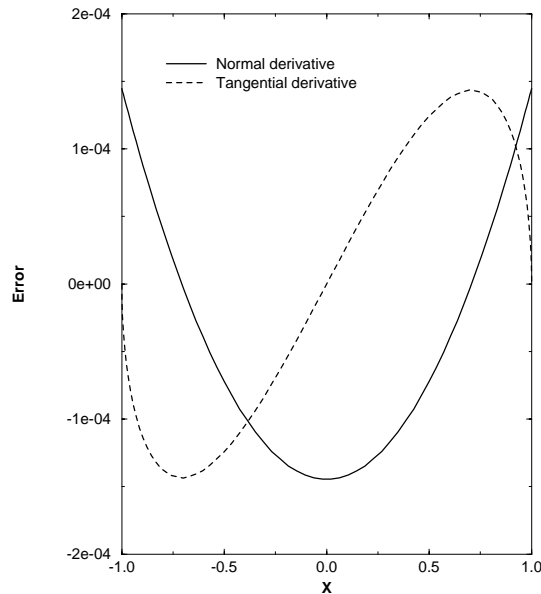


Figure 1: The errors in the calculated normal and tangential components of  $\nabla\phi$ , for the solution of Laplace’s equation on the unit disk with Dirichlet boundary conditions.

More or less standard boundary integral techniques can be used to approximate and solve Eq. (5). Various direct and regularization methods have been developed for treating the hypersingular integral within a collocation approximation, Gray, Martha and Ingraffea 1990; Guiggiani 1993; Krishnasamy, Rizzo and Rudolphi 1991; Tanaka, Sladek and Sladek 1994. In this work the singular Galerkin integrals are evaluated using a combined analytical and numerical approach, Gray 1998. These techniques are similar to the collocation techniques presented in Gray 1993.

As a preliminary test of this method, Laplace's equation was solved on the unit disk, with Dirichlet boundary values  $\phi = x^2 - y^2$ . The exact gradient on the surface is  $\nabla\phi = (2x, -2y)$ . Fig. 1 displays the errors in the computed normal (Laplace solution) and tangential (post-processing solution) derivatives. As the solutions are symmetric, only the results of the bottom half of the unit circle are shown. Note that the error in the tangential component is of the same order of magnitude as the error in the initial solution. This calculation, and those reported in the next section, employed a linear element Symmetric Galerkin approximation, Hartmann, Katz and Protosaltis 1985.

## Boundary Corners

As mentioned briefly in the introduction, previous methods for evaluating surface derivatives have serious difficulties at boundary corners and edges. For direct collocation of a hypersingular integral at a corner point, existence of the integral requires that the interpolation of the potential *and* the normal flux be consistent (Gray and Lutz 1990; Gray and Manne 1993). This constraint is the analogue of the smooth surface  $C^1$  condition, and while it can be incorporated in the approximation, it is not a simple matter, Gray 1994. It is possible that the 'displacement gradient' method can compute values at a corner, but existing implementations appear to be valid only for smooth surfaces, Okada, Rajiyah and Atluri 1988, pg. 789. As a consequence, this approach computes derivatives at nodes shifted away from the corner.

The flexibility provided by the choice of weight function allows a simple treatment of corners within the Galerkin method. In two dimensions, the corner is represented by the usual technique of a 'double node' pair, one node for each side of the corner. A tangential derivative equation for each node is obtained by specifying that the weight function  $\psi_k$  be non-zero on only one side of the corner. Thus, the two corner nodes have different, non-overlapping, weight functions, and the system of linear equations is non-singular. Another consequence of this procedure is that the equations 'terminate' at a corner: since the product of the two shape functions at the corner is zero, there is no matrix element connecting the two tangential derivative values. This is potentially very useful for applications which do not require knowledge of the derivative everywhere on the boundary.

As a simple example, the Dirichlet problem discussed above has been solved on the unit square, employing a uniform grid spacing of 0.05. The calculated values for both normal and tangential derivatives at the corners are shown in Table 2. These results indicate that the method can accurately determine the multiple values at a corner. Note that in this case the tangential values are more accurate than the computed normal derivatives.

corner point	Normal Derivative		Tangential Derivative	
	Calculated	Exact	Calculated	Exact
(0.0 <sup>+</sup> , 0.0)	0.03458	0.00000	0.01488	0.00000
(0.0, 0.0 <sup>+</sup> )	-0.03458	0.00000	0.01488	0.00000
(1.0 <sup>-</sup> , 0.0)	0.03376	0.00000	1.98500	2.00000
(1.0, 0.0 <sup>+</sup> )	1.96531	2.00000	-0.01467	0.00000
(1.0, 1.0 <sup>-</sup> )	1.96613	2.00000	-1.98521	-2.00000
(1.0 <sup>-</sup> , 1.0)	-1.96613	-2.00000	-1.98521	-2.00000
(0.0 <sup>+</sup> , 1.0)	-1.96531	-2.00000	-0.01467	0.00000
(0.0, 1.0 <sup>-</sup> )	-0.03376	0.00000	1.98500	2.00000

Table 1: Calculated normal and tangential derivatives at the corners of the unit square for the solution of Laplace’s equation with Dirichlet boundary values  $\phi = x^2 - y^2$ .

Apparently, this is not uncommon, Guiggiani 1993.

### 3 Electric Fields on Voids in Interconnects Under Electromigration Conditions

In this section, Eq. (5) is applied to a problem of practical interest, electromigration-induced failure in metallic thin-film interconnects. Tangential derivative solutions are shown to be in excellent agreement with finite-element simulations employing refined meshes.

As electronic device sizes keep decreasing toward ultra-large scale integration (ULSI), mechanical failure in Al-based thin film interconnects presents a serious reliability challenge. Open-circuit failure due to void propagation is a common failure mechanism in accelerated electromigration testing experiments. Void nucleation occurs during thin film thermal processing and subsequent void growth and migration take place during circuit operation. A simple geometry for a two-dimensional simulation of electromigration-induced void dynamics is shown in Fig. 2. The model domain,  $-\infty < x < \infty$ ,  $0 \leq y \leq W$ , consists of a strip representing an Al thin film in a solid state device which has been damaged by the formation of a void. The dynamics of a void under the action of external forces, such as applied electric fields, mechanical loads, and thermal stresses (Maroudas, Enmark, Leibig and Pantelides 1995), is of utmost importance in the context of interconnect failure. Here, the interaction of the void with an imposed electric field is considered.

A boundary integral approach is particularly appealing for simulating electromigration-

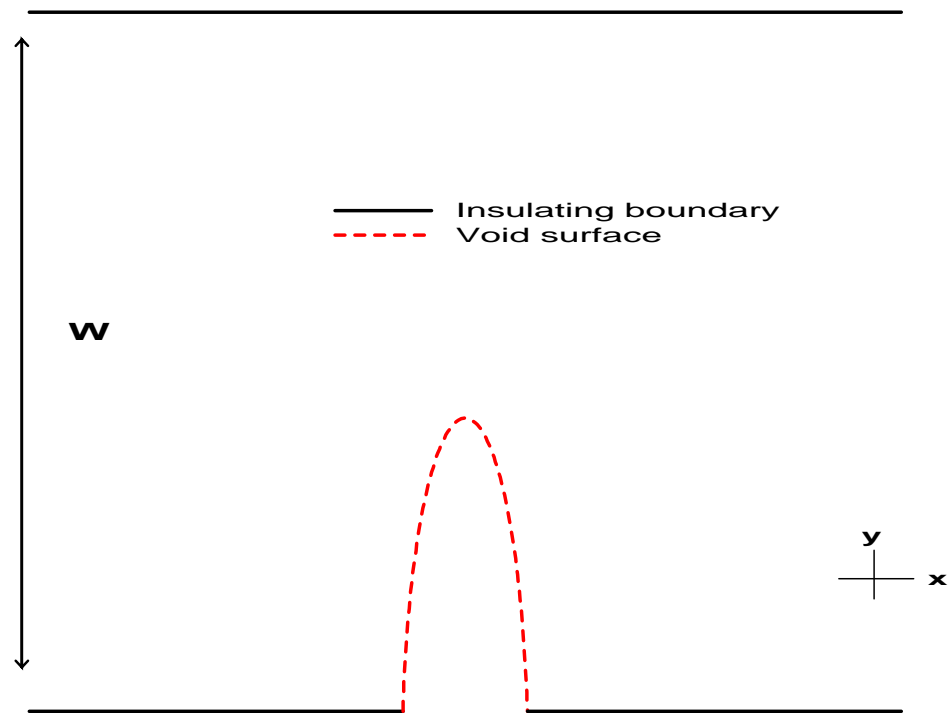


Figure 2: A two dimensional model for a damaged interconnect film, consisting of a strip of infinite length and width  $W$  (solid line) containing a void defect (dashed line).

induced void dynamics. First, only surface quantities, such as the tangential component of the electric field  $\mathbf{E}$ , are needed for the simulation. This is due to the fact that, for the materials involved and the temperature range of interest, surface diffusion is a much faster process than diffusion in the film away from the void surface (Bower and Freund 1995; Maroudas 1995; Maroudas and Pantelides 1995). Thus, only surface diffusional processes, such as surface electromigration, need to be considered. Moreover, with the Galerkin algorithm, surface derivatives can be evaluated directly (*i.e.*, without finite difference approximations) and, as indicated by Fig. 1, as accurately as the initial solution of the differential equation.

Second, as the void surface evolves, re-discretization of the domain is considerably easier for a boundary method. In fact, the boundary integral calculation can be formulated so that only the void surface is input to the calculation. In this case, the only remeshing required would be when the transformed grid on the void no longer produces an accurate solution, *e.g.*, nodes drifting apart. A 'void only' simulation is achieved by replacing the point source potential, Eq. (3), by a Green's function which exactly satisfies the zero-flux boundary condition on the  $y = 0$  strip boundary and closely approximates this condition on  $y = W$  (Gray, Maroudas, Enmark and D'Azevedo). This permits the removal of these surfaces from the calculation, as all integrals over the strip in Eq. (1) and Eq. (2) vanish or nearly vanish. In addition to simplifying the solution to Laplace's equation, this is also convenient for the post-processing computation of the tangential derivatives. The strip boundaries are no longer present, and thus limiting the derivative calculation to the void surface is no longer an issue.

Let  $\Phi(x, y)$  denote the electrostatic potential, so that  $\mathbf{E} = -\nabla\Phi$  is the electric field (or potential flux) and, since  $\mathbf{E}$  is solenoidal and irrotational,  $\nabla^2\Phi = 0$ . The boundary conditions are zero normal flux on the insulating strip boundaries and on the void surface, together with an imposed electric field  $\mathbf{E} = (E_\infty, 0)$  at infinity, *i.e.*, far away from the void surface. It is convenient to reformulate the problem by defining the potential  $\phi$  via

$$\Phi = -E_\infty x + \phi , \quad (6)$$

so that  $\phi$  vanishes at infinity. Note that the boundary conditions for  $\phi$  remain zero normal flux on the strip boundaries, where  $\mathbf{n} = (n_x, n_y) = (0, \pm 1)$ , while on the void surface

$$\nabla\phi \cdot \mathbf{n} = E_\infty n_x . \quad (7)$$

The electric field contribution to the flux of atoms on the void surface is proportional to the tangential component,

$$E_s = -\nabla\Phi \cdot \mathbf{T} = -\nabla\phi \cdot \mathbf{T} + E_\infty t_x , \quad (8)$$

where  $\mathbf{T} = (t_x, t_y)$  is the unit tangent vector on the void. Once the surface atomic flux is known, the void velocity normal to the void surface can be computed from the surface divergence,  $\partial E_s / \partial s$ , where  $s$  indicates the arclength measured along the void surface. The void surface can then be advanced in time, and the process repeated with the new geometry. A method for calculating  $\partial E_s / \partial s$  within the boundary integral formulation will be presented in a forthcoming publication (Maroudas, Enmark, Gray and D’Azevedo).

The boundary integral solution for  $\phi$  is obtained using a linear element symmetric Galerkin approximation, Hartmann, Katz and Protosaltis 1985. As the boundary condition on the void is specified flux, using the flux equation, Eq. (2), in conjunction with a Galerkin formulation results in a symmetric coefficient matrix.

To validate the Galerkin technique, the results of the boundary element (BEM) tangential derivative calculations are compared to corresponding computations carried out with the finite element method (FEM). The FEM solution to Laplace’s equation utilized an 8-noded serendipity element, and a finite domain of length  $L$  in the  $x$  direction, the void placed in the middle of the domain. The value of  $L$  was determined by a series of convergence tests to guarantee that the application of the far-field condition at the ends of the finite domain does not affect the quantitative accuracy of the computations. In all cases,  $L = 12W$  was found to be satisfactory. The FEM meshes are graded very finely near the void surface where high potential gradients are expected, and along the void surface for accurate evaluation of the tangential component of  $\mathbf{E}$ . Typically, the number of degrees of freedom involved in the FEM simulations is on the order of  $10^4$ . In the BEM calculations discussed below, the number of nodes on the void is 101.

In the first set of calculations, the tangential derivative is determined for an initial void shape and three subsequent perturbations of this shape, which are shown in Fig. 3. The width of the interconnect in these calculations is  $W = 3.0$ , and thus the void is well separated from the top boundary. The initial shape is a circular arc, which corresponds to the steady solution for  $E_\infty = 0$ . The other three void morphologies are steady state solutions as  $E_\infty$  increases from zero. These steady solutions correspond to a zero surface flux divergence for given values of  $E_\infty$  and involve solving the nonlinear surface diffusion and electromigration problem coupled self-consistently with the electric field. The details of the self-consistent solution scheme for void morphological stability analyses under electromigration conditions will appear elsewhere. The results of the calculations, shown in Fig. 4, are in excellent agreement with the finite element solutions.

A second set of steady void morphologies and the corresponding void surface solutions for the tangential component of  $\mathbf{E}$  are displayed in Figs. 5 and 6. In this case, however, the width of the strip is  $W = 0.5$ ; thus, the void spans roughly 80% of the interconnect in the  $y$  direction. For such geometries, the electric field computation becomes more difficult for

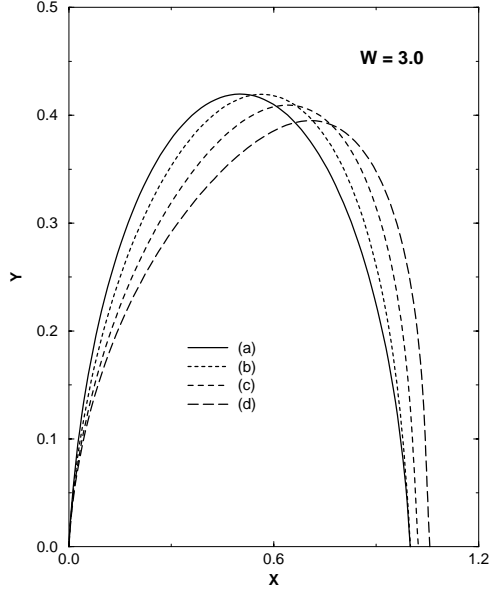


Figure 3: Four steady void shapes in an Al strip of width  $W = 3.0$ . The length scale is set by the size of void (a) in the direction of the electric field. The void volume (area in this two-dimensional model) is conserved as the void morphology changes.

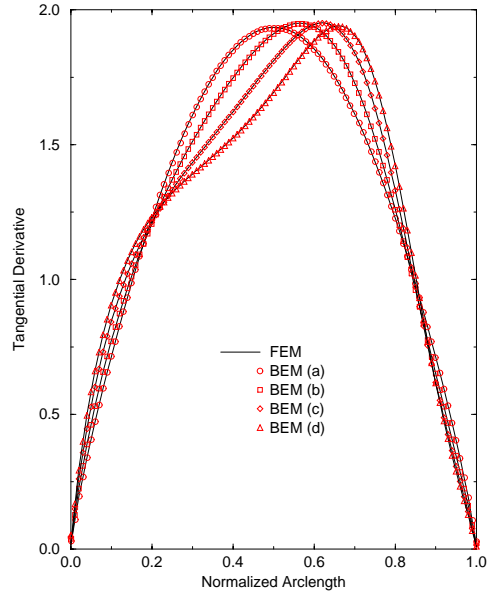


Figure 4: Comparison between the tangential derivative calculations using the FEM and BEM methods for the voids shown in Fig. 3. The tangential derivative curves (a) – (d) correspond to the shapes in Fig. 3.

both finite element and boundary element methods. The magnitude of the electric field near the top of the void is much higher and the electric field gradients are much steeper in this case. Once again, the results from both methods match very well.

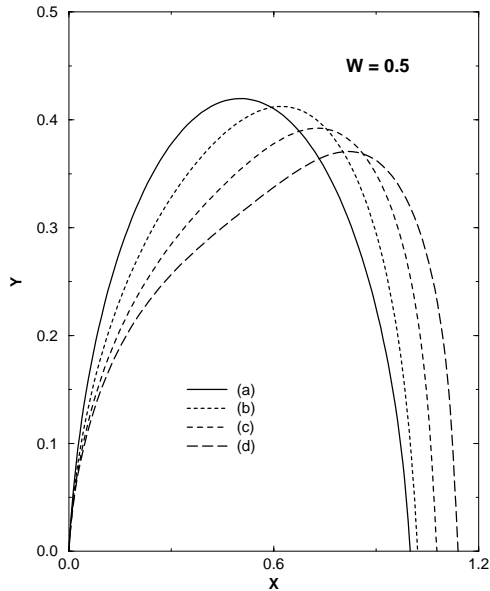


Figure 5: Four steady void shapes in an Al strip of width  $W = 0.5$ . Again, the void area is conserved.

## 4 Conclusions

A Galerkin algorithm for the post-processing evaluation of tangential derivative values has been shown to produce highly accurate results. The primary advantages of this technique are that *nodal* derivative values are obtained directly and accurately, evaluation of the hypersingular equation is carried out with standard  $C^0$  boundary interpolations, and that corners and edges present no difficulties. These three features should make this approach attractive for most applications.

The development of this method was motivated by a problem of technological interest, electromigration-driven void dynamics in metallic thin films. Although this application involved the solution of the two-dimensional Laplace equation, there is no difficulty in extending this work to either three dimensions or other equations. In particular, evaluation of the surface stress tensor presents no additional difficulties.

The boundary derivatives are determined by solving a system of linear algebraic equations,

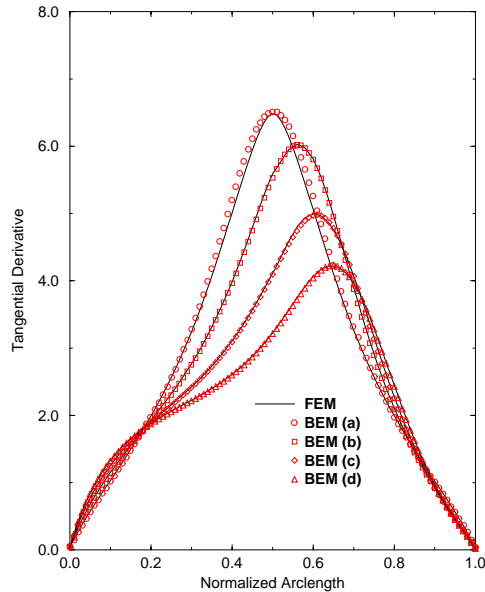


Figure 6: Comparison between the tangential derivative calculations using the FEM and BEM methods for the voids shown in Fig. 5. The tangential derivative curves (a) – (d) correspond to the shapes in Fig. 5.

and as a consequence the initial formulation requires that these values be obtained everywhere on a smooth connected segment of the boundary. The fact that the Galerkin method is not a single point algorithm is a potentially serious drawback of the method, as it may pose an unacceptable computational burden in some applications. If the derivative is only needed on a small portion of a segment, then given expense of computing the right hand side in Eq. (5), computing derivatives on an entire segment could easily become too time consuming. Preliminary tests indicate that the system of equations can be truncated to a ‘slightly enlarged’ region of interest, with little loss of accuracy. However, this truncation scheme is a rather crude approximation, and further work is required to determine a more effective method for terminating the system of equations.

## Acknowledgment

This research was supported by the Applied Mathematical Sciences Subprogram, Office of Basic Energy Sciences, U.S. Department of Energy, under contract DE-AC05-84OR21400 with Martin Marietta Energy Systems Inc., by the Laboratory Directed Research and Development Program of the Oak Ridge National Laboratory, by the National Science Foundation through a CAREER Award to DM (ECS-95-01111), and by the National

Science Foundation under grant PHY94-07194 with the Institute for Theoretical Physics (ITP), University of California, Santa Barbara. L.J.G. gratefully acknowledges the hospitality of the ITP, where part of this work was carried out.

## References

- [1] Bower, A. F. and Freund, L. B. (1995): Finite element analysis of electromigration and stress induced diffusion in deformable solids. In: Oates, A. S. Filter, W. F., Rosenberg, R., Greer, A. L. and K. Gadepally (eds.): *Materials Reliability in Microelectronics V*, vol. 391, pp. 177–188. Pittsburgh: Materials Research Society.
- [2] Cruse, T. A. and Van Buren, W. (1971): Three-dimensional elastic stress analysis of a fracture specimen with an edge crack. *Int. J. Fracture Mechanics* 7, pp. 1–15.
- [3] Fiedler, C. (1995): On the calculation of boundary stresses with the Somigliana identity. *Int. J. Numer. Meth. Engrg.* 38, pp. 3275–3295.
- [4] Gray, L. J. (1991): Evaluation of hypersingular integrals in the boundary element method. *Math. Comp. Modelling* 15, pp. 165–174.
- [5] ———(1993): Symbolic computation of hypersingular boundary integrals. In: Kane J. H., Maier, G., Tosaka, N., and Atluri, S. N. (eds.): *Advances in boundary element techniques*, pp. 157–172. Berlin: Springer-Verlag.
- [6] ———(1994): A note on Overhauser elements. *Boundary Element Comm.* 5, pp. 62–65.
- [7] ———, (1998): Evaluation of Galerkin singular integrals. In: Sladek, V. and Sladek, J. (eds.): *Singular Integrals in the Boundary Element Method*. Southampton: Computational Mechanics (in press).
- [8] Gray, L. J. and Lutz, E. D. (1990): On the treatment of corners in the boundary element method. *J. Comp. Appl. Math.* 32, pp. 369–386.
- [9] Gray, L. J. and Manne, L. L. (1993): Hypersingular boundary integrals at a corner: *Engrg. Analy. Boundary Elem.* 11, pp. 327–334.
- [10] Gray, L. J., Maroudas, D., Enmark, M. N. and D’Azevedo, E. F. Approximate Green’s functions in boundary integral analysis. in preparation.
- [11] Gray, L. J., Martha, L. F. and Ingraffea, A. R. (1990): Hypersingular integrals in boundary element fracture analysis. *Int. J. Numer. Meth. Engrg.* 29, pp. 1135–1158.

- [12] Guiggiani, M. (1993): Hypersingular integral equations and superaccurate stress evaluation. In: Brebbia, C. A. and Rencis, J. J. (eds.): *Boundary Elements XV*, vol. 1, pp. 413–428. Southampton: Computational Mechanics Publications.
- [13] Guiggiani, M., Krishnasamy, G., Rudolphi, T. J. and Rizzo, F. J. (1992): A general algorithm for the numerical solution of hypersingular boundary integral equations. *ASME J. Appl. Mech.* 59, pp. 604–614.
- [14] Hartmann, F., Katz, C. and Protopsaltis, B. (1985): Boundary elements and symmetry. *Ingenieur-Archiv* 55, pp. 440–449.
- [15] Hildenbrand, J. and Kuhn, G. (1992): Numerical computation of hypersingular integrals and application to the boundary integral equation for the stress tensor. *Engrg. Analy. Boundary Elem.* 10, pp. 209–217.
- [16] Kane, J. H. (1994): *Boundary Element Analysis in Engineering Continuum Mechanics*. New Jersey: Prentice Hall.
- [17] Krishnasamy, G., Rizzo, F. J. and Rudolphi, T. J. (1991): Hypersingular boundary integral equations: Their occurrence, interpretation, regularization and computation. In: Banerjee, P. K. and Kobayashi, S. (eds.): *Developments in Boundary Element Methods - Advanced Dynamic Analysis*, vol. 7, ch. 7. London: Elsevier Applied Science Publishers.
- [18] Lutz, E. D. and Gray, L. J. (1993): Exact evaluation of singular boundary integrals without CPV, *Comm. Num. Meth. Engrg.* 9 pp. 909–915.
- [19] Lutz, E. D., Gray, L. J. and Ingraffea, A. R. (1990): Indirect evaluation of surface stress in the boundary element method. In: Morino, L. and Piva, R. (eds.): *Boundary Integral Methods: Theory and Applications*. Berlin: Springer Verlag.
- [20] Maroudas, D. (1995): Dynamics of transgranular voids in metallic thin films under electromigration conditions. *Appl. Phys. Lett.* 67, pp. 798–800.
- [21] Maroudas, D., Enmark, M. N., Gray, L. J. and D’Azevedo, E. F. Morphological stability and dynamics of voids in metallic thin-film interconnects under electromigration conditions. in preparation.
- [22] Maroudas, D., Enmark, M. N., Leibig, C. M. and Pantelides, S. T. (1995): Analysis of damage formation and propagation in metallic thin films under the action of thermal stresses and electric fields. *J. Computer-Aided Materials Design* 2, pp. 231–258.

- [23] Maroudas, D. and Pantelides, S. T. (1995): Theory and computer simulation of grain boundary and void dynamics in polycrystalline conductors. In: Oates, A. S. Filter, W. F., Rosenberg, R., Greer, A. L. and K. Gadepally (eds.): *Materials Reliability in Microelectronics V*, vol. 391, pp. 151–162. Pittsburgh: Materials Research Society.
- [24] Martin, P. A. and Rizzo, F. J. (1989): On boundary integral equations for crack problems. *Proc. R. Soc. Lond. A421*, pp. 341–355.
- [25] ———, Hypersingular integrals: how smooth must the density be? *Int. J. Numer. Meth. Engrg.* 39, pp. 687–704.
- [26] Matsumoto, T. Tanaka, M. and Hirata, H. (1993): Boundary stress calculation using regularized boundary integral equation for displacement gradients. *Int. J. Numer. Meth. Engrg.* 36, pp. 783–797.
- [27] Okada, H., Rajiyah, H. and Atluri, S. N. (1988): A novel displacement gradient boundary element method for elastic stress analysis with high accuracy. *Trans. ASME*, 55, pp. 786–794.
- [28] ———, Non-hypersingular integral representations for velocity (displacement) gradients in elastic/plastic solids (small or finite deformations). *Comp. Mech.* 4, pp. 165–175.
- [29] Rizzo, F. J. and Shippy, D. J. (1968): A formulation and solution procedure for the general non-homogeneous elastic inclusion problem. *Int. J. Solids Struct.* 4, pp. 1161–1173.
- [30] Rudolphi, T. J. (1989): Higher order elements and element enhancement by combined regular and hypersingular boundary integral equations. In: Annigeri, B. S. and Tseng, K. (eds.): *Boundary Element Methods in Engineering*, pp. 448-455. Berlin: Springer Verlag.
- [31] Sladek, V. and Sladek, J. (1986): Improved computation of stresses using the boundary element method. *Appl. Math. Modelling* 10, pp. 249–255.
- [32] Tanaka, M., Sladek, V. and Sladek, J. (1994): Regularization techniques applied to boundary element methods. *Appl. Mech. Reviews* 47, pp. 457–499.
- [33] Watson, J. O. (1986): Hermitian cubic and singular elements for plain strain. In: Banerjee, P. K. and Watson, J. O. (eds.): *Developments in Boundary Element Methods*, Vol. 4, pp. 1–28. London: Elsevier Applied Science Publishers.
- [34] Zhao, Z. (1997): On the calculation of boundary stresses in boundary elements. *Engrg. Anal. Boundary Elem.* 16, pp. 317–322.